

# The Structure of Polyunsaturated Lipid Bilayers Important for Rhodopsin Function: A Neutron Diffraction Study

Mihaela Mihailescu\* and Klaus Gawrisch<sup>†</sup>

\*Department of Physiology and Biophysics, University of California, Irvine, California; and <sup>†</sup>Laboratory of Membrane Biochemistry and Biophysics, National Institute on Alcohol Abuse and Alcoholism, National Institutes of Health, Bethesda, Maryland 20892

**ABSTRACT** The structure of oriented 1-stearoyl-2-docosahexaenoyl-*sn*-glycero-3-phosphocholine bilayers with perdeuterated stearoyl- or docosahexaenoyl hydrocarbon chains was investigated by neutron diffraction. Experiments were conducted at two different relative humidities, 66 and 86%. At both humidities we observed that the polyunsaturated docosahexaenoyl chain has a preference to reside near the lipid water interface. That leaves voids in the bilayer center that are occupied by saturated stearoyl chain segments. This uneven distribution of saturated- and polyunsaturated chain densities is likely to result in membrane elastic stress that modulates function of integral receptor proteins like rhodopsin.

Received for publication 29 July 2005 and in final form 21 September 2005.

Address reprint requests and inquiries to Klaus Gawrisch, E-mail: [gawrisch@helix.nih.gov](mailto:gawrisch@helix.nih.gov).

Lipids containing the sixfold unsaturated docosahexaenoic acid ((DHA) 22:6n3) are found at high concentrations in brain synaptosomes and the retina. They are essential for the development of the human brain (1). It had been suggested that polyunsaturation alters membrane properties that are critical for activity of integral receptor proteins (2). Therefore, exploring the structure of polyunsaturated bilayers is a prerequisite for understanding how neural membranes function. Here it is demonstrated that distribution of saturated and polyunsaturated hydrocarbon chains differs significantly, supporting the hypothesis that DHA-containing membranes are under considerable elastic stress that may influence the function of integral membrane proteins.

The lipid 1-stearoyl-2-docosahexaenoyl-*sn*-glycero-3-phosphocholine (18:0-22:6-PC) was synthesized (Avanti Polar Lipids, Alabaster, AL) with specifically deuterated stearoyl (SA)—or DHA chains (Martek, Columbia, MD). The DHA chain was deuterated to 38% except for the terminal methyl group that was deuterated to 30%, as determined by <sup>2</sup>H NMR. Oriented bilayers were prepared by application of 1–2 mg of 18:0-22:6-PC dissolved in methylene chloride to glass coverslips. The solvent was removed in a stream of N<sub>2</sub> gas. Samples contained the antioxidant BHT at a lipid/BHT molar ratio of 100:1 and were prepared and investigated in an oxygen-free environment. Less than 1000 bilayers per slide were applied to guarantee low mosaicity and negligible neutron extinction effects.

The measurements were performed at either 66 or 86% relative humidity, created by enclosing small containers with saturated salt solution (NaNO<sub>2</sub> or KCl) in the sample chamber filled with argon. The distribution of saturated and polyunsaturated hydrocarbon chains was determined by <sup>1</sup>H-<sup>2</sup>H contrast variation. Diffraction experiments were performed on the advanced neutron diffractometer/reflectometer (3) at the NIST Center for Neutron Research, Gaithersburg, MD.

The diffraction data were collected in a  $\theta$ – $2\theta$  (specular) mode. Eight orders of diffraction were observed (Fig. 1). The coherent, diffracted intensity at each Bragg order was determined by integrating the counts under the peaks after background subtraction as well as absorption and Lorentz factor corrections (4). The structure factors  $F(n)$  are then determined—up to a phase factor—as the square root of the peak integrals. Phases were determined by analyzing H<sub>2</sub>O–<sup>2</sup>H<sub>2</sub>O exchange experiments. A plot of structure factors as a function of <sup>2</sup>H<sub>2</sub>O content of the water of hydration yielded a linear dependence that enabled phase assignment for all Bragg peaks, except the eighth order that had too low intensity for an unambiguous assignment (see Fig. 1s in Supplementary Material). However, because of its low intensity, the influence of this uncertainty on the resulting density profiles was not significant. Finally, the distribution of scattering length densities (SLD) was obtained by Fourier synthesis of the structure factors. The large differences in SLD between protonated and deuterated hydrocarbon chains permitted calculation of the SLD distribution of saturated and polyunsaturated chains (Fig. 2). The uncertainty bands associated with the density profiles in Fig. 2 were determined from the standard deviations in the experimental structure factors, including uncertainties in the scale factors, by a Monte-Carlo sampling procedure.

Repeat distances of  $52 \pm 0.2$  Å and  $52.3 \pm 0.2$  Å at relative humidities of 66 and 86%, respectively, were measured. Neutron extinction effects appeared as a nonlinearity of structure factors versus <sup>2</sup>H<sub>2</sub>O content of the low- $Q$ , high-intensity diffraction peaks (mainly for  $n = 1$ ), (5). Only the sample with two protonated hydrocarbon chains at 86% relative humidity required a correction. The method of Wiener and White (6) was used to determine an absolute (per lipid)

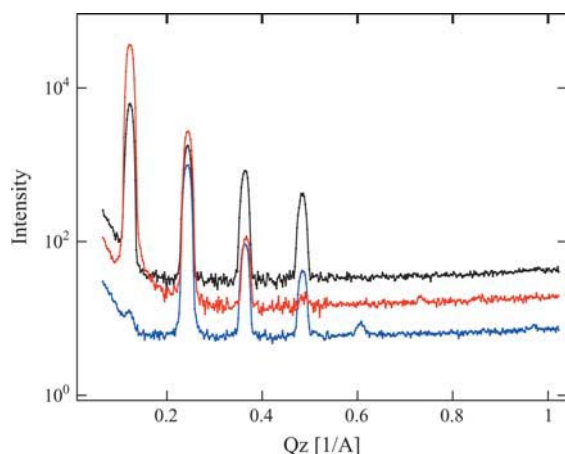


**FIGURE 1** Diffraction data of 18:0-22:6-PC oriented multilayers, with protonated hydrocarbon chains (*black*), with deuterated stearoyl chains (*orange*), or with deuterated DHA chains (*blue*).

scale of SLD (up to an unknown constant  $S$ , accounting for the area per lipid; Fig. 2.) The scaling factors were determined from the measurements conducted as a function of  $^2\text{H}_2\text{O}$  content. The mean SLDs per lipid were calculated based on a water content 6.1 and 9.4 waters per lipid at 66 and 86% relative humidity, respectively (7). The SA chain SLD peaked in the middle of the bilayer whereas the polyunsaturated chain SLD was highest near the lipid water interface. Please note that the lower SLD of DHA results mostly

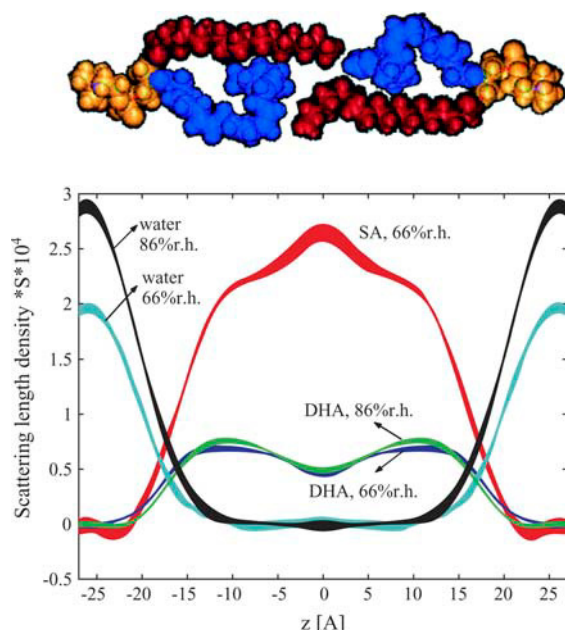


**FIGURE 2** Scattering length density distributions of lipid hydrocarbon chains and water calculated as density difference of bilayers with protonated and deuterated hydrocarbon chains. The line width reflects the uncertainty bands. The SLDs reflect higher densities of DHA (*blue*) near the lipid water interface and of SA (*red*) in the bilayer center as shown in the model above the graph.

from the lower degree of deuteration (38%  $^2\text{H}$  in  $-\text{CH}_2-$  and  $=\text{CH}-$  and 30% in  $-\text{CH}_3$ ).

The broad trough seen in the DHA chain SLD is mostly the result of a lower probability of DHA chain segments to reside in the bilayer center. This was confirmed by calculations using a realistic DHA chain distribution function from molecular dynamics simulations (see Fig. 2s in Supplementary Material) (8). The contribution from the somewhat lower level of deuteration of the terminal methyl groups was negligible. In contrast, the SA chain has a SLD maximum in the bilayer center. Other bilayers, such as di-unsaturated 18:1-18:1-PC (DOPC) (9) or mixed chain saturated-mono-unsaturated 16:0-18:1-PC POPC (M. Mihailescu, unpublished data) do not have such a SLD maximum but a trough that was explained by the larger volume of terminal  $\text{CH}_3$  groups compared to  $\text{CH}_2$ . Therefore, the SLD maximum of SA in 18:0-22:6-PC bilayers reflects higher probability of SA chain segments to reside in the bilayer center, compared to the saturated palmitic acid chain in POPC bilayers. Obviously, the SA chains fill the voids that are left by lower DHA chain density in this region. Some dynamic interdigitation of SA chains from the two apposing monolayers of the bilayer may contribute to higher SA density as well.

The water density profile in Fig. 2 is an envelope over the total water hydrating two opposing bilayers. It could be approximated by a sum of two Gaussian distributions (Fig. 3s in Supplementary Material). The changes in chain density distributions from an increase in relative humidity were minor. However, the water distribution broadened and water molecules penetrated deeper into the bilayers at higher relative humidity.

These findings are in excellent agreement with NMR and x-ray diffraction measurements as well as molecular simulations conducted at full hydration that suggest a somewhat uneven distribution of chain densities (8). However, in contrast to previous results the neutron diffraction experiments are a direct, quantitative measure of this unevenness. The conclusion is that segments of the polyunsaturated DHA chains have a higher probability to locate near the water-lipid interface whereas the segments of saturated chains are more likely to reside in the bilayer center. The order of saturated stearic acid chain segments near the terminal methyl group, measured by  $^2\text{H}$  NMR (8,10), is lower because those chain segments are on average more tilted to the bilayer normal to fill the voids from a lower probability of DHA segments to reside in the bilayer center. This uneven distribution of saturated and polyunsaturated chains is likely to alter the lateral pressure profile of bilayers that has been linked to changes in free energy of activated G-protein coupled membrane receptors, like rhodopsin, upon conversion to the activated state (11).

## SUPPLEMENTARY MATERIAL

An online supplement to this article can be found by visiting BJ Online at <http://www.biophysj.org>.

## ACKNOWLEDGMENTS

We thank Scott E. Feller for providing the molecular dynamics simulation results of chain density distribution in 18:0-22:6-PC bilayers and Stephen H. White for helpful discussions.

The AND/R, constructed by the Cold Neutrons for Biology and Technology (CNBT) partnership, is supported by the National Institute of Standards and Technology, the Regents of the University of California, and by a grant from the National Institute for Research Resources awarded to the University of California at Irvine. K.G. is supported by the Intramural Research Program of the National Institutes of Health, National Institute on Alcohol Abuse and Alcoholism.

## REFERENCES and FOOTNOTES

1. Salem, N., B. Litman, H. Y. Kim, and K. Gawrisch. 2001. Mechanisms of action of docosahexaenoic acid in the nervous system. *Lipids*. 36:945–959.
2. Cantor, R. S. 1999. Lipid composition and the lateral pressure profile in bilayers. *Biophys. J.* 76:2625–2639.
3. <http://www.ncnr.nist.gov/programs/reflect/ANDR>. [Online].
4. Worcester, D. L., and N. P. Franks. 1976. Structural analysis of hydrated egg lecithin and cholesterol bilayers. II. Neutron diffraction. *J. Mol. Biol.* 100:359–378.
5. Bacon, G. E., and R. D. Lowde. 1948. Secondary extinction and neutron crystallography. *Acta. Crystallogr.* 1:303–314.
6. Wiener, M. C., G. I. King, and S. H. White. 1991. Structure of a fluid dioleoylphosphatidylcholine bilayer determined by joint refinement of x-ray and neutron diffraction data. I. Scaling of neutron data and the distributions of double bonds and water. *Biophys. J.* 60: 568–576.
7. Binder, H., and K. Gawrisch. 2001. Dehydration induces lateral expansion of polyunsaturated 18:0–22:6 phosphatidylcholine in a new lamellar phase. *Biophys. J.* 81:969–982.
8. Eldho, N. V., S. E. Feller, S. Tristram-Nagle, I. V. Polozov, and K. Gawrisch. 2003. Polyunsaturated docosahexaenoic vs docosapentaenoic acid: differences in lipid matrix properties from the loss of one double bond. *J. Am. Chem. Soc.* 125:6409–6421.
9. Wiener, M. C., and S. H. White. 1992. Structure of a fluid dioleoylphosphatidylcholine bilayer determined by joint refinement of x-ray and neutron diffraction data. II. Distribution and packing of terminal methyl groups. *Biophys. J.* 61:428–433.
10. Petrache, H. I., A. Salmon, and M. F. Brown. 2001. Structural properties of docosahexaenoyl phospholipid bilayers investigated by solid-state  $^2\text{H}$  NMR spectroscopy. *J. Am. Chem. Soc.* 123:12611–12622.
11. Carillo-Tripp, M., and S. E. Feller. 2005. Evidence for a mechanism by which  $\omega$ -3 polyunsaturated lipids may affect membrane protein function. *Biochemistry*. 44:10164–10169.